



Theoretical investigation on the non-covalent interactions of acetaminophen complex in different solvents: study of the enhancing effect of the cation- π interaction on the intramolecular hydrogen bond

Marziyeh Mohammadi¹ · Azadeh Khanmohammadi²

Received: 28 April 2020 / Accepted: 21 July 2020 / Published online: 6 August 2020
© Springer-Verlag GmbH Germany, part of Springer Nature 2020

Abstract

In the current research, a comprehensive study is performed on the non-covalent interactions of the acetaminophen complex in the presence of various solvents. In addition, the effect of cation- π interaction on the strength and nature of the intramolecular hydrogen bond (H-bond) is explored by density functional theory method. The computations are performed using the M06-2X functional and the 6-311++G(d,p) basis set. The obtained results reveal that both interactions become stronger in the gas phase with respect to the solution phase. The “atoms in molecules” theory and the natural bond orbital method are also applied to get more details about the investigated interactions character. Based on the achieved outcomes, the H-bond of the studied complex is placed in the weak H-bond category. Our findings indicate that the intramolecular H-bond is strengthened by the cation- π interaction in the different solvents. Finally, the physical properties such as frontier molecular orbitals, energy gap, dipole moment, chemical hardness as well as electronic chemical potential are investigated to evaluate the electronic properties, stability and reactivity of the studied complex.

Keywords Acetaminophen · Cation- π · Hydrogen bond · AIM · NBO

1 Introduction

Acetaminophen (*N*-acetyl-*p*-aminophenol [APAP], paracetamol) is a medication that has good analgesic and antipyretic properties [1, 2]. It was first made in 1877 [3]. Acetaminophen (AC) is available as a generic medication with trade names of Tylenol and Panadol [4]. It has relatively little anti-inflammatory activity [5–7] unlike other common analgesics such as aspirin and ibuprofen. In general, AC is less efficacious than salicylates and other antirheumatic agents

for problems that require anti-inflammatory treatment. AC overdose may be manifested by renal tubular necrosis, hypoglycemic coma and thrombocytopenia. Sometimes, liver necrosis can occur as well as liver failure [8]. One theory is that AC increases the pain threshold by inhibiting two isoforms of cyclooxygenase, COX-1 and COX-2, which are involved in prostaglandin (PG) synthesis. Prostaglandins are responsible for eliciting pain sensations [9]. AC does not inhibit cyclooxygenase in peripheral tissues. It blocks COX indirectly [10].

Non-covalent interactions are originated from interactions between a permanent dipole and an induced dipole or from an instantaneous time variable multipole and an induced multipole [11]. These interactions may be a combination of several interactions such as ion pairing, H-bonding, π - π interactions and cation- π interactions [12–16]. They determine material properties, orchestrate chemical reactions, drive molecular recognition and are active in the regulation of biochemical processes [17, 18]. The H-bond is the most popular form of non-covalent interactions, which is formed between a hydrogen atom attached to an electronegative

Electronic supplementary material The online version of this article (<https://doi.org/10.1007/s00214-020-02650-8>) contains supplementary material, which is available to authorized users.

✉ Marziyeh Mohammadi
m.mohammadi@vru.ac.ir

¹ Department of Chemistry, Faculty of Science, Vali-e-Asr University of Rafsanjan, P. O. Box: 77176, Rafsanjan, Iran

² Young Researchers and Elite Club, Quchan Branch, Islamic Azad University, Quchan, Iran

donor atom and a neighboring acceptor atom. It is a relatively strong non-covalent interaction (4–120 kJ/mol). The H-bonded complexes are stabilized by electrostatic, induction (charge transfer) and dispersion energy terms. The electrostatic term is composed of dipole–dipole and dipole–charge interactions. It is the most important energy term and it gives to H-bonds their directionality [19, 20]. The concept of H-bonds has been extended to C–H...Y (Y = electronegative atom) and C–H... π types of H-bonds [11, 21]. These interactions are several kJ/mol weaker than classical H-bonds [22], but they are believed to be crucial driving forces in crystal packing [23] and in molecular recognition [24, 25]. The cation– π interaction, as another ensemble of non-covalent interactions, implies the attraction of a cation to the electron density associated with a π -system [26]. Strong forces are found between cations and a π -face of an aromatic ring [27]. The energy value related to the cation– π interactions is variable (5–80 kJ/mol). Electrostatic forces play a dominant role in the cation– π interaction, but also induced dipole, polarizability, dispersion and charge transfer terms are involved.

Understanding the non-covalent interactions and the interplay among them are of pivotal importance to the development of fields such as supramolecular chemistry and molecular recognition [28–30]. The interplay between non-covalent interactions can be favorable or unfavorable depending on the nature of the aromatic ring and the sign of the ion. The simultaneous presence of these interactions in a complex leads to the cooperativity effects that are helpful for understanding some biological processes [31]. Many research studies have been devoted to the study of the interplay between cation– π interactions and H-bonding [32–35]. There are many synergetic effects in complexes where these interactions exist. Experimental evidence [36] has also been reported from synergetic effects between several non-covalent interactions.

In recent years, it has become clear that interactions with metal ions are important factors in the modes of action of many drugs. The importance of understanding the nature of the drugs interactions with metals which may be present in body fluids is now beyond dispute [37]. Our study focuses on the structure and relative stability of acetaminophen drug with a Fe^{2+} bivalent cation having partially filled valence d orbitals. The selection of this transition metal ion mainly comes from the important role that it plays in biochemical processes [38–40]. This ion interacts with the drug due to the increased electrostatic potential and smaller ionic radius in comparison with the non-transition metal ions [40, 41]. On the other hand, the function of biologically active molecules depends on their structure and interaction with the solvent, which affects biological processes [42]. In 2013, Issa et al. investigated the effects of iron on the pharmacokinetics of acetaminophen in saliva [43]. It has been

reported that AC can be chelated with iron [44]. Sunagane et al. [45] found that no in vitro reaction between ferrous ion and AC and combined administration of AC and iron showed no influence on bioavailability of AC. In addition, other studies have shown that there is an aerobic (in the gastrointestinal tract) oxidation of ferrous ion to ferric ion caused in iron–AC in vivo reactions [46, 47]. As a result, the simultaneous administration of iron decreases the extent of absorption of AC and very slightly increases its rate of absorption [43].

It is also noteworthy to mention that the formed complexes between transition metal cations with aromatic hydrocarbons have been considered in various contexts. For example, Demircan et al. [48] investigated the structures and interaction energies for complexes formed by Fe^{2+} , Co^{2+} , Ni^{2+} , Cu^{2+} and Zn^{2+} binding with benzene molecules in a wide range of methods and basis sets. The results displayed strong bindings between transition metal cations and benzene molecules. Further, in a 2009 study, Yi et al. demonstrated that transition metal cation– π interactions also include covalent characters due to π donations [48, 49]. In 2002, the structural and electronic effects of the interaction of transition metal cations with benzene analyzed using quantum chemical calculations by Dobado et al. [50]. A theoretical investigation of the cation– π interactions in complexes of benzene (Bz) with cations, that is, $\text{M}^{z+}(\text{Bz})_n$ for $\text{M}^{z+} = \text{Na}^+$, Mg^{2+} , Fe^{2+} and $n = 1–3$ was also conducted in 2014 [51]. However, transition metal cations are more challenging for quantum chemical methods than main group cations since most of them have open-shell electronic structures [48].

Our objectives are divided in four parts. The first aim is based on a theoretical study to investigate the influence of cation– π interaction on the stability, binding energy and some structural and electronic properties of the AC complex in the different solvents. The second section determines the geometrical parameters, topological properties, population analysis and H-bond strength of the related complex to gain further insight into the intramolecular H-bond interaction in the selected solvents. The third goal of the evaluation of the AC complex is to explore the effect of cation– π interaction on H-bond properties. The last part refers to comprehensive analysis of these interactions on HOMO–LUMO data.

2 Computational details

In this work, all computations are performed with Gaussian 03 program [52] at the M06-2X level of theory using the 6-311++ $G(d,p)$ (385 basis functions and 623 primitive Gaussians) basis set. This method has been proved to be reliable for the study of non-covalent complexes [53–57]. The calculations are carried out in the presence of several

different solvents (water, methanol, ethanol, ether, chloroform and acetone) using the self-consistent reaction field (SCRf) method with the polarized continuum model (PCM) [58]. The nature of optimized geometries for local minima is checked with frequency calculations. In this study, the intramolecular H-bond energy is estimated by means of the Espinosa method [59]. In addition, the binding energy with and without the basis set superposition error (BSSE) [60] correction is calculated than the geometrical optimizations. For the analyzed system, the binding energy can be evaluated from difference between the energy of complex and the sum of energies of the isolated species. The following equation is applied to calculate this energy:

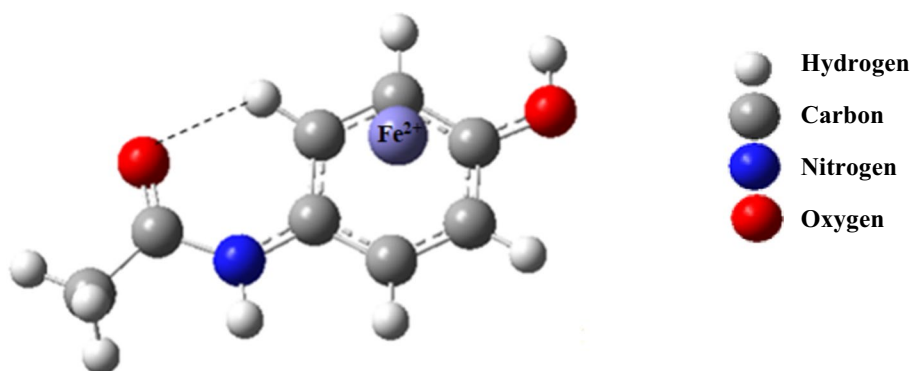
$$\Delta E = E_{\text{cation}-\pi} - (E_{\text{cation}} + E_{\pi\text{-system}}) \quad (1)$$

Based on this formula, $E_{\text{cation}-\pi}$ is the total energy of complex and E_{cation} and $E_{\pi\text{-system}}$ are referred to the total energies of isolated cation and acetaminophen monomer, respectively. The selected complex stability is also explored in the presence of various solvents and their results are compared with together and also with the gas phase. The stabilization energy (E_{stab}) can be evaluated by the following equation:

$$E_{\text{stab}} = E_{\text{tot}}(\text{solvent}) - E_{\text{tot}}(\text{gas}) \quad (2)$$

where $E_{\text{tot}}(\text{solvent})$ and $E_{\text{tot}}(\text{gas})$ are the total energy of system in the presence and in the absent of different solvents, respectively. The AIM analysis [61] is carried out using the AIM2000 program [62] generally from wave function obtained at the M06-2X/6-311++G(d,p) level of theory. The charge transfer in complex is also calculated by the natural bond orbital (NBO) method [63] using NBO program [64] under Gaussian 03 program package. Other interesting theoretical studies are related to the highest occupied molecular orbital (HOMO) and the lowest unoccupied molecular orbital (LUMO) energies obtained at the same level of theory to represent the electronic properties, stability and reactivity of the selected complex.

Fig. 1 Optimized structure of AC...Fe²⁺ complex at the M06-2X/6-311++G(d,p) level of theory



3 Results and discussions

3.1 Cation- π interaction

Figure 1 illustrates the full optimized structure of acetaminophen complex (AC...Fe²⁺) at the M06-2X/6-311++G(d,p) level of theory. Fe²⁺ is an open-shell system, with a d^6 configuration, and there are three different spin states (singlet, triplet and quintet). The low-spin (LS) state is the singlet and the high-spin (HS) state the quintet [51]. In this study, because the spin multiplicity of the AC-Fe²⁺ complex is considered the singlet, it is the low spin. The most important geometrical parameters are reported in Table 1. It can be stated that with the exception of AC complex in the gas phase, our computations show a reverse relationship between $|\Delta E|$ and $d_{\text{ion}-\pi}$ (the distance among the ion and the middle of aromatic ring) values for the analyzed complex. According to Table 1, the maximum and minimum $d_{\text{ion}-\pi}$ values belong to the polar and nonpolar solvents, respectively. Theoretical results also demonstrate that the increment in the C=C bond length ($d_{\text{C=C}}$) upon complexation is associated with increasing $|\Delta E|$ values, so that the degree of elongation of the double bond (C=C) is higher for the nonpolar solvents than the polar ones (see Table 1).

Table 1 Geometrical parameters of cation- π (bond lengths (d) in Å), binding energies without and with the BSSE correction (ΔE and ΔE^{corr} in kJ/mol) and dielectric constant (ϵ) of the solvents

Media	$d_{\text{C=C}}$	$d_{\text{ion}-\pi}$	ΔE	ΔE^{corr}	ϵ
Water	1.415	1.762	-27.51	-21.22	80.0
Methanol	1.416	1.756	-36.87	-30.71	32.7
Ethanol	1.416	1.755	-42.59	-36.17	24.5
Acetone	1.417	1.754	-47.80	-41.34	20.7
Chloroform	1.421	1.736	-156.68	-151.87	4.81
Ether	1.422	1.727	-175.03	-168.75	4.33
Gas phase	1.428	1.737	-836.44	-833.71	-

The calculated binding energies without and with the BSSE correction (ΔE and ΔE^{corr}) are given in Table 1. Based on PCM results, the binding energies of the investigated system considerably change in the presence of different solvents. Probe of results indicates that the binding energy of complex in the solution phase is lower than the obtained value in the gas phase. Table 1 shows that the $d_{\text{ion}-\pi}$ of the studied system changes appreciably when solvent effects are taken into account. For $d_{\text{ion}-\pi}$, an increase in distances is observed in going from the gas phase to the solution. Hence, the binding energy of the AC complex drops from $-833.71 \text{ kJ mol}^{-1}$ in the gas phase to -168.75 and $-21.22 \text{ kJ mol}^{-1}$ in the ether (as a nonpolar solvent) and in the water (as a polar solvent), respectively. However, Table 1 shows that the highest/lowest binding strength is related to the nonpolar/polar solvents. The trend in the achieved binding energy values in different solvents is as follows:

water < methanol < ethanol < acetone < chloroform < ether

As can be seen, the formation of AC complex in ether with higher binding energy is energetically more favorable than the other solvents. Our findings show a meaningful

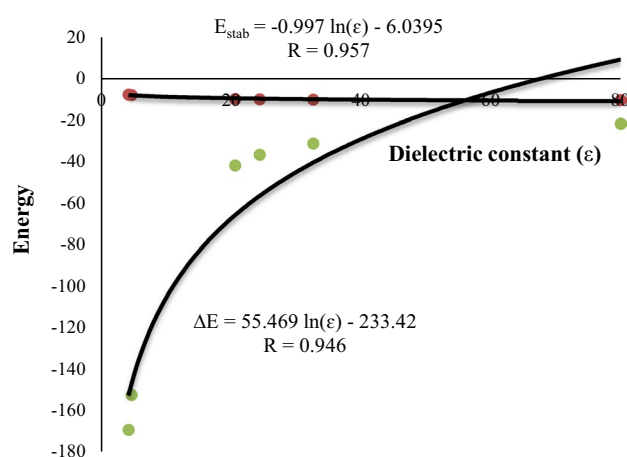


Fig. 2 Relationship between ΔE and E_{stab} versus solvent dielectric constant (ϵ)

relationship between the obtained binding energies and dielectric constant (ϵ) of the solvents. This dependency is shown in Fig. 2. It is worth mentioning that with the increase in the dielectric constant or polarity of the solvent, the binding energy shifts to lower values (see Table 1). The solvent affects the potential energy surface and is dependent on it, and polarity stabilizes the related complex [65].

The computations also suggest that the type of solvent plays an important role in determining the stability of the AC complex. The values of stability energy in the different solvents are given in Table 2. Based on the obtained results, the stability in water is the most ($\approx -9.91 \text{ eV}$), and in ether, it is the least ($\approx -7.25 \text{ eV}$). In fact, the negative values of the E_{stab} show that the solvent leads to stabilization. Table 2 also shows that the calculated E_{stab} in the AC complex is considerably higher than its corresponding monomer. Similar to the obtained E_{stab} for the AC monomer, it can also be seen in different possible conformers of AC investigated by Yoosefian et al. [65]. This can attribute to large relatively binding energies of the related complex in the different solvents. In AC monomer, the E_{stab} depends only on the solvation energy, while in the AC complex, in addition to the solvation energy, the intermolecular binding energy also affects the E_{stab} . It is well known that the computed binding energies for transition metal cations are significantly stronger (~ 4 – 11 times) compared with main group metal cations [66]. Figure 2 presents that the stability energy correlates with the dielectric constant, while its correlation coefficient R amounts to 0.957. This plot displays that the dielectric constants decay exponentially as the stability energy increases.

For AC complex in the various solvents, the dependence between the binding and stability energies is also considered. The results show an excellent linear relationship between the related energies. The corresponding correlation coefficient is equal to 0.995. Therefore, ΔE could be easily evaluated from E_{stab} as: $\Delta E = -82.639 E_{\text{stab}} - 812.87$. As it is apparent, the increase in E_{stab} is associated with decreasing ΔE in the selected solvents. According to these results, it can be stated that although AC complex has the least binding energy in the polar solvents, its stability in these solvents is more than

Table 2 Values of total energy, relative energy and stability energy (E_{stab}) of the AC monomer and its complex in the gas phase and different solvents

	Monomer			Complex		
	Total energy (E_{tot} , Hartree)	Relative energy (E_r , eV)	E_{stab} (eV)	Total energy (E_{tot} , Hartree)	Relative energy (E_r , eV)	E_{stab} (eV)
Water	-515.2753	-0.0155	-0.4221	-1778.5030	-0.3644	-9.9124
Methanol	-515.2747	-0.0150	-0.4071	-1778.4941	-0.3555	-9.6698
Ethanol	-515.2744	-0.0147	-0.3995	-1778.4896	-0.3510	-9.5479
Acetone	-515.2742	-0.0144	-0.3928	-1778.4856	-0.3471	-9.4400
Chloroform	-515.2703	-0.0106	-0.2874	-1778.4143	-0.2757	-7.5002
Ether	-515.2698	-0.0101	-0.2740	-1778.4051	-0.2665	-7.2496
Gas phase	-515.2597	0.0000	0.0000	-1778.1386	0.0000	0.0000

the others. Hence, the stability energy could be major factor to estimate the strength of these interactions.

The quantum theory of atoms in molecules (QTAIM) [61, 67] is an intent to rigorously define the atom and chemical bond from the polyelectronic wave function. Principally being based on Hellman–Feynman theorem [68], it shows that all properties of one molecule are determined by the electron density distribution (ρ) and its second derivative ($\nabla^2\rho$) at the bond critical point (BCP). These properties are often applied as descriptors of cation– π interaction. In the AIM theory, strong shared-shell interatomic interactions (such as covalent bonding) are characterized by local concentration of charge ($\nabla^2\rho(r) < 0$), and thus, the BCPs of covalent bonds have the large ρ and negative $\nabla^2\rho(r)$, whereas weak closed-shell interactions (such as hydrogen bonding, ionic bonds and van der Waals interactions) exhibit local depletion of charge ($\nabla^2\rho(r) > 0$) and the BCPs of them have the small ρ and positive $\nabla^2\rho(r)$.

The obtained topological parameters for AC complex in the gas phase and the different solvents are given in Table 3. The determined electron density properties for $\text{AC}\cdots\text{Fe}^{2+}$ complex demonstrate that the ρ_{BCP} has low values (ranging from 0.0587 to 0.0669) and the $\nabla^2\rho_{\text{BCP}}$ values are positive (ranging from 0.1813 to 0.2229). This means that the related

complex has specification of the closed-shell interactions in nature. The introduction of various solvents causes the significant changes in the topological properties upon complexation. According to the average of the calculated topological parameters in Table 3, it is clear that the enhancement of electron density at BCP (ρ_{BCP}) of the nonpolar solvents is associated with the decline of that in the polar ones. These results also confirm outcomes based on the geometrical data and the binding energies. In other words, the shorter distance ($d_{\text{ion}-\pi}$) and larger electron density (ρ_{BCP}) at ion $\cdots\pi$ contact are accompanied with greater strength of cation– π interaction.

The obtained results in Tables 1 and 3 also show that the increment in $|\Delta E|$ value is accompanied with the decrease in $\rho_{\text{C}=\text{C}}$ value. A reverse relationship also exists between the $\rho_{\text{C}=\text{C}}$ value and its corresponding bond length. The molecular graph and the computed contour map of AC complex using the AIM2000 program package are shown in Fig. 3. As it is apparent, the $\text{AC}\cdots\text{Fe}^{2+}$ complex is characterized by bond critical points formed between the Fe^{2+} metal cation and each carbon atom of AC ring. Because the studied complex shows high relatively binding energy and low geometrical deformation in its structure, there are only four BCPs between the metal and the carbon atoms. Similar to the

Table 3 Topological properties of electron density (in a.u.) calculated at the M06-2X/6-311++G(d,p) level of theory

	Water	Methanol	Ethanol	Acetone	Chloroform	Ether	Gas phase
ρ_{BCP}	0.0600	0.0604	0.0604	0.0605	0.0626	0.0635	0.0669
	0.0598	0.0604	0.0606	0.0607	0.0625	0.0630	0.0599
	0.0604	0.0611	0.0613	0.0615	0.0638	0.0631	0.0587
	0.0596	0.0602	0.0602	0.0603	0.0626	0.0645	0.0655
$\nabla^2\rho_{\text{BCP}}$	0.1813	0.1832	0.1835	0.1837	0.1907	0.1906	0.2067
	0.2009	0.2036	0.2048	0.2057	0.2187	0.2076	0.1855
	0.1939	0.1960	0.1966	0.1970	0.2025	0.2223	0.1927
	0.1933	0.1950	0.1954	0.1958	0.2056	0.2030	0.2229
$\rho_{\text{C}=\text{C}}$	0.2968	0.2964	0.2962	0.2961	0.2936	0.2931	0.2894

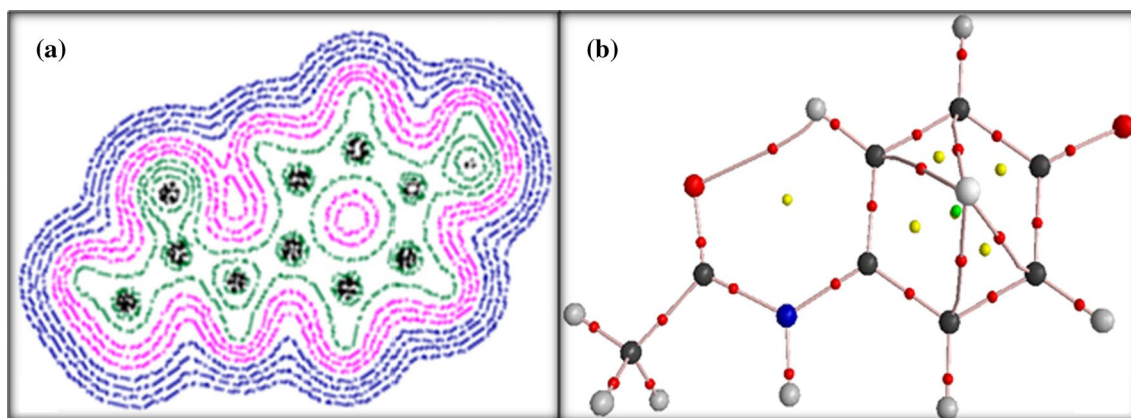


Fig. 3 a Contour map and b molecular graph of $\text{AC}\cdots\text{Fe}^{2+}$ complex obtained from M06-2X/6-311++G(d,p) wave function

AC complex, it can also be seen on the formed complexes between transition metal cations with benzene [50].

The NBO analysis is able to describe the atomic components of bonding. It is also possible using second-order perturbation theory ($E^{(2)}$) to calculate the strength the donor–acceptor interaction based on all of the intuitive means for describing the interaction, such as orbital occupancy, overlap and energy difference [63]. The results of NBO analysis demonstrate that the donor–acceptor interaction energies, $E^{(2)}$, reported in Table 4 are related to dominant interaction of $\pi_{(C-C)} \rightarrow LP^*_{(cation)}$ which is between π -electrons of donor species and LP^* of the cation as acceptor agent. As observed in this table, the donor–acceptor energy of the mentioned interaction decreases on passing from the gas phase to the solution phase. This trend is identical with $|\Delta E|$. Table 4 also represents the values of NBO occupation number calculated at the M06-2X/6-311++G(d,p) level of theory. Our findings show that, in most cases, the reduction (enhancement) in occupation number of donor (acceptor) orbitals is accompanied with the increase in $|\Delta E|$, ρ_{BCP} , $E^{(2)}$ and also, the diminish in $\rho_{C=C}$ value (see Tables 1, 3 and 4).

The values of charge transfer ($\Delta q_{(CT1)}$) for the AC complex are displayed in Table 5. The transferred charge between the AC ring and Fe^{2+} cation during complexation could be easily found as the difference of charges between free cation and complexed cation. Table 5 shows that the largest charge transfer occurs in the nonpolar solvents, while the smallest that corresponds to the polar ones. For instance, the charge

transfer for the AC complex in gas phase is 0.812, which decreases to 0.524 and 0.324 in the ether and water solvents (see Table 5), respectively. Hence, the charge transfer values in the studied complex also confirm that the interaction in solution phases is weaker than the gas phase. In addition, the results indicate that the increase in $|\Delta E|$ value is associated with the increment in value of $\Delta q_{(CT1)}$ upon complexation. Therefore, the charge transfer may be a useful parameter for describing the strength of ion- π interactions.

3.2 Intramolecular hydrogen bond

In this part, we intend to investigate the H-bond strength of AC complex in the various solvents and its result compares with the gas phase. Yoosefian et al. [65] performed DFT computational study on solvent effect, molecular conformations, energies and intramolecular H-bond strength in different possible nano-conformers of AC. They showed that from 4 different obtained conformers for AC, the represented structure in Fig. 1 is the most stable one with intramolecular C–H...O H-bonding. The optimized geometrical parameters of complex are presented in Table 6. It is well known that these parameters can be considered as one of the indicators of H-bond strength [69]. For a stronger H-bond, this kind of complexation usually results in the elongation of the C–H bond length as proton donor and the shortening of the O...H distance as proton acceptor. The achieved results demonstrate that the O...H distance ($d_{O...H}$) and the C–H bond length (d_{C-H}) are in the ranges of 2.093–2.146 Å and

Table 4 NBO analyses of AC complex including occupation numbers of donor (O.N._D) and acceptor (O.N._A) orbitals and their energies (in kcal/mol) of some important orbitals

Media	$\pi_{C-C} \rightarrow LP^*_{cation}$			$LP_O \rightarrow \sigma^*_{C-H}$		
	O.N. _D	O.N. _A	$E^{(2)}$	O.N. _D	O.N. _A	$E^{(2)}$
Water	1.5924	0.2840	42.50	1.9765	0.0146	0.90
Methanol	1.5924	0.2860	42.94	1.9764	0.0146	0.93
Ethanol	1.5924	0.2864	42.99	1.9764	0.0147	0.94
Acetone	1.5925	0.2868	43.06	1.9764	0.0147	0.95
Chloroform	1.5947	0.2937	45.27	1.9758	0.0150	1.10
Ether	1.5937	0.2951	45.97	1.9757	0.0151	1.17
Gas phase	1.5783	0.3096	45.97	1.9747	0.0141	1.22

Table 5 Results of natural bond orbital analysis and the charge transfers (Δq_{CT} in e) at the M06-2X/6-311++G(d,p) level of theory

Media	Occ Val _O	(%S) of LP _O	q_O	$\Delta q_{(CT1)}$	$\Delta q_{(CT2)}$
				$\pi_{C-C} \rightarrow LP^*_{cation}$	$LP_O \rightarrow \sigma^*_{C-H}$
Water	6.5328	58.49	−0.358	0.324	0.082
Methanol	6.5327	58.42	−0.353	0.343	0.084
Ethanol	6.5326	58.38	−0.350	0.353	0.085
Acetone	6.5326	58.35	−0.347	0.361	0.087
Chloroform	6.5304	57.78	−0.310	0.500	0.100
Ether	6.5319	57.74	−0.305	0.524	0.102
Gas phase	6.5104	56.10	−0.203	0.812	0.142

Table 6 Geometrical parameters of H-bond (bond length (d) in Å), topological parameters (in a.u.), H-bond energy (E_{HB} in kJ/mol) and dipole moment (μ° in Deby) of the AC complex in different solvents

Media	$d_{\text{C-H}}$	$d_{\text{O}\cdots\text{H}}$	$\rho_{\text{O}\cdots\text{H}}$	$\nabla^2\rho_{\text{O}\cdots\text{H}}$	$H_{\text{O}\cdots\text{H}}$	E_{HB}	μ°
Water	1.079	2.146	0.0201	0.0788	0.0023	-19.81	11.17
Methanol	1.079	2.141	0.0203	0.0797	0.0023	-20.07	10.93
Ethanol	1.079	2.139	0.0204	0.0802	0.0023	-20.22	10.81
Acetone	1.079	2.136	0.0204	0.0806	0.0023	-20.33	10.71
Chloroform	1.080	2.110	0.0214	0.0858	0.0024	-21.84	9.15
Ether	1.080	2.101	0.0218	0.0874	0.0024	-22.34	8.83
Gas phase	1.082	2.093	0.0219	0.0901	0.0026	-22.75	5.01

1.079–1.082 Å, respectively (see Table 6). As revealed in this table, the $d_{\text{O}\cdots\text{H}}$ in the gas phase is less than the solution phase. This trend is reversed for the $d_{\text{C-H}}$. The results show that these parameters in the ether and chloroform solvents are closed to the gas phase, because the dielectric constant of them is small.

In the present paper, the H-bond energies (E_{HB}) could be estimated from the properties of bond critical points. The simple relationship between H-bond energy and the potential energy density $V(\text{rcp})$ at the critical point corresponding to $\text{O}\cdots\text{H}$ contact is assigned to be $E_{\text{HB}} = 1/2 V(\text{rcp})$ [59, 70, 71]. According to Table 6, the H-bond strength of AC complex in the gas phase is higher than the solution phase, and in the polar solvents, it is lower than the nonpolar ones. The trend of the H-bond strength in different solvents is as follows:

water < methanol < ethanol < acetone < chloroform < ether

As it can be observed, the H-bond is the strongest for the ether solvent and the weakest for the water solvent. This outcome can also be supported by the shorter $d_{\text{O}\cdots\text{H}}$ and the larger $d_{\text{C-H}}$ of this complex in the ether solvent with respect to the other ones. There are remarkable relationships between the H-bond energies and the obtained geometrical parameters. For instance, the linear correlation coefficients for the dependence between E_{HB} versus $d_{\text{O}\cdots\text{H}}$ and $d_{\text{C-H}}$ are equal to 0.999 and 0.883, respectively, with an equation as follows:

$$E_{\text{HB}} = -965.58 (56.043) d_{\text{C-H}} (d_{\text{O}\cdots\text{H}}) + 1021.5 (-140.07)$$

Besides the geometrical and energetic analyses, the theory of atoms in molecules is also applied in the analysis of H-bonds [72–76]. As shown in Fig. 3, the place of the bond critical point strongly depends on electronegativity, so that the situation of BCP is located closer to electropositive atom. This leads to the increase in the BCP electronegative atom distance and decrease in the BCP electropositive atom distance. The results of AIM analysis indicate that the values of charge density at the BCP of $\text{O}\cdots\text{H}$ ($\rho_{\text{O}\cdots\text{H}}$) increase as: gas phase > ether > chloroform > acetone \approx ethanol > methanol > water. Based on our theoretical results, this order is same as the achieved results by H-bond energies

(see Table 6). The Laplacian sign is also used as a criterion for the H-bond strength [77, 78]. The positive and negative signs of the calculated values refer to weak and strong H-bond interactions, respectively. The calculated electron density properties display that the $\text{O}\cdots\text{H}$ bonding has low ρ values and $\nabla^2\rho$ of positive. These results confirm that H-bond of the studied complex is placed in the weak H-bond category. The theoretical results also prove that the order of $\nabla^2\rho$ values at BCP of $\text{O}\cdots\text{H}$ is in accordance with the H-bond energy order (see Table 6).

A good feature of the NBO method is that it provides interesting information about the electron density transfer in donor \rightarrow acceptor interactions [63]. The NBO calculations also confirm the presence of $\text{C-H}\cdots\text{O}$ H-bond in the AC complex. It should be mentioned that significant interaction of $\text{LP}_\text{O} \rightarrow \sigma^*_{\text{C-H}}$ occurs between LP_O and $\sigma^*_{\text{C-H}}$ in the studied complex. The LP_O participates as donor, and $\sigma^*_{\text{C-H}}$ acts as acceptor. The interaction between bonding and antibonding molecular orbitals can be found by the second-order perturbation interaction energy, $E^{(2)}$ [79–82]. The results of NBO analysis are given in Table 4. As shown in this table, the obtained $E^{(2)}$ values lie in the range of 0.9–1.22 kcal mol $^{-1}$. The greatest and smallest $E^{(2)}$ values at the M06-2X/6-311++G(d,p) level of theory belong to the nonpolar and polar solvents, respectively. A reverse relationship also exists between the $E^{(2)}$ and LP_O occupancy values. Our results reveal that the greater LP_O occupancy is accompanied with the lowest $E^{(2)}$ value and vice versa. The outcomes also demonstrate that the occupation number of donor (O.N. $_D$) and acceptor (O.N. $_A$) orbitals for the AC complex in the polar solvents is approximately the same and does not change considerably (see Table 4); as a result, the polar solvents have a relatively low effect on the H-bond of AC complex.

The values of Val_O occupation number in the different solvents are also explored. Our findings reveal that the Val_O occupancy in the gas phase is equal to 6.5104 e. As given in Table 5, the Val_O is enhanced in the presence of various solvents. The NBO analysis is also applied for investigating of the hybridization of LP_O corresponding to sp^n in the AC complex. The results show that the s character of this orbital is also increased by different solvents (see Table 5).

The increase in s character leads to a decrease in the Lewis base (O atom) properties of AC. For the studied complex, a linear relationship is found among $E^{(2)}$ and LP_O hybridization value (see Fig. 4).

Table 5 also shows the values of charge transfer ($\Delta q_{(CT2)}$) obtained for the AC complex. As shown in this table, the highest charge transfer belongs to the AC complex in the nonpolar solvents, whereas the lowest that corresponds to the polar ones. In fact, the greater charge density on oxygen atom (q_O) leads to the more charge transfer of AC complex. Furthermore, comparing the values of $E^{(2)}$ and E_{HB} versus the $\Delta q_{(CT2)}$ shows a direct relationship between them (see Tables 4, 5, 6). Thus, the charge transfer may be a valuable factor for depicting the strength of H-bond interactions.

In the present study, we have considered the dipole moment (μ°) of AC complex in both the gas phase and solvent media (see Table 6). Our findings show that the greatest dipole moments belong to polar solvents, whereas the smallest ones correspond to nonpolar solvents. The achieved computations propose that the dissimilarity between the dipole moments can be related to the character of different solvents. Indeed, the increase in the dipole moment in the polar solvents may be explained by consideration of the charge value on the oxygen atom (q_O) with high electronegativity. It is worth mentioning that in the AC complex, the oxygen atom carries the highest/lowest negative charge in the polar/non-polar solvents (see Table 5). On the other hand, the least and most positive charge exists on the hydrogen atom (involved in H-bond) of the polar and nonpolar solvents, respectively (data not reported). Therefore, the existence of the electronegative element in complex makes possible its interaction with the hydrogen atom through H-bonding formation.

3.3 The effect of cation- π interaction on the C-H...O H-bond

Because the objective of this section is to evaluate the cation- π interaction effect on the strength and nature of the

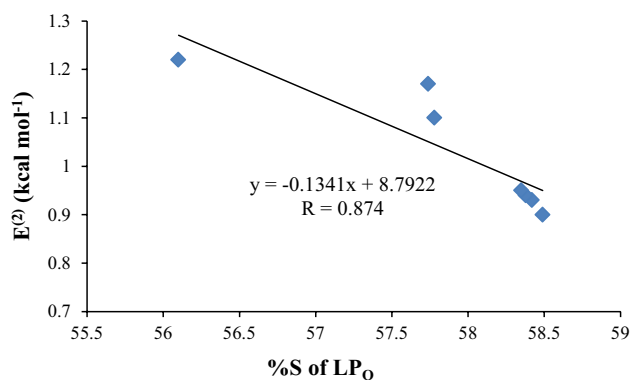


Fig. 4 $E^{(2)}$ value of $LP_O \rightarrow \sigma^*_{C-H}$ interaction versus %S of LP_O

C-H...O intramolecular H-bond, we only focus on the complex geometries which optimized in fixed $d_{ion-\pi}$ (achieved at previous section). It can be stated that with the exception of AC complex in the gas phase, a direct relationship can be found between the equilibrium distances at both cation- π ($d_{ion-\pi}$) and H-bond ($d_{O...H}$) interactions. This means that both interactions become stronger in the nonpolar solvents in comparison with the polar ones (see Tables 1 and 6). As shown in these tables, this outcome can also be confirmed by the obtained energies. In other words, our data prove that the order of calculated binding energies (ΔE) is in accordance with the estimated H-bond energies (E_{HB}) order. However, the theoretical results based on the binding energies predict the strongest cation- π interaction for the AC...Fe²⁺ complex in the gas phase. Thus, the related complex in the gas phase has a stronger influence on the H-bond with respect to the solution phase, which is consistent with study of the previous sections.

The $d_{O...H}$ values presented here may be compared with $|\Delta E|$ (see Tables 1 and 6). The obtained data show that the increment in $|\Delta E|$ is associated with decreasing $d_{O...H}$. The dependence of $d_{O...H}$ to ion- π interactions can also be investigated using q_O . The increasing $d_{O...H}$ in the selected complex may be due to the decrease in q_O in the presence of cation (see Tables 5 and 6). Thus, the $d_{O...H}$ changes of complex may be dependent on the q_O changes in the different solvents.

Theoretical results also indicate that the maximum/minimum value of $\rho_{O...H}$ is accompanied with the highest/lowest $|\Delta E|$ in the studied complex (see Tables 1 and 6). However, it can be stated that the AC complex has the values of more $\rho_{O...H}$ and higher $|\Delta E|$ in the gas phase in comparison with the solution phase. On the other hand, in case of the various solvents, the highest of these values belong to the nonpolar solvents with respect to the polar ones. Tables 1 and 4 show that the $E^{(2)}$ energy value of corresponding to H-bond enhances with increasing $|\Delta E|$ in the considered complex. The result of calculations also reveals that the increase in the charge transfer ($\Delta q_{(CT2)}$) upon complexation is in agreement with the increment of $|\Delta E|$ value. From the obtained results, it can be concluded that the strength of H-bond of AC complex increases by cation- π interaction in the presence of different solvents.

3.4 Electronic properties

Molecular orbitals (HOMO and LUMO) and its energy gap are very useful parameters in quantum chemistry. They are applied by the frontier electron density for predicting the most reactive position in π -electron systems and also explain several types of reaction in conjugated system [83]. Localization of electron density in HOMO advocates that the particular site is nucleophilic, whereas the site for LUMO is

electrophilic in nature [84]. The energy gap between HOMO and LUMO is a critical parameter in determining molecular electrical transport properties [85]. It explains the biological activity [86] of the molecule, which is due to the change in partial charge and total dipole moment [87, 88].

To understand the bonding scheme of $AC \cdots Fe^{2+}$ complex, the frontier orbitals for the titled complex in the gas phase are drawn and are illustrated in Fig. 5. As observed, the positive and negative phases are red and green, respectively. For this complex, the energy values of HOMO and LUMO and its energy gap are computed -16.98 , -11.30 and 5.68 eV, respectively. These orbitals importantly overlap in the gas phase and decreasing energy gap between HOMO and LUMO explains the eventual charge transfer interaction taking place within the molecule. Figure 5 shows that in the titled complex, both the HOMO and LUMO are more localized on aromatic ring. Moreover, there is no electronic projection over other parts of this complex.

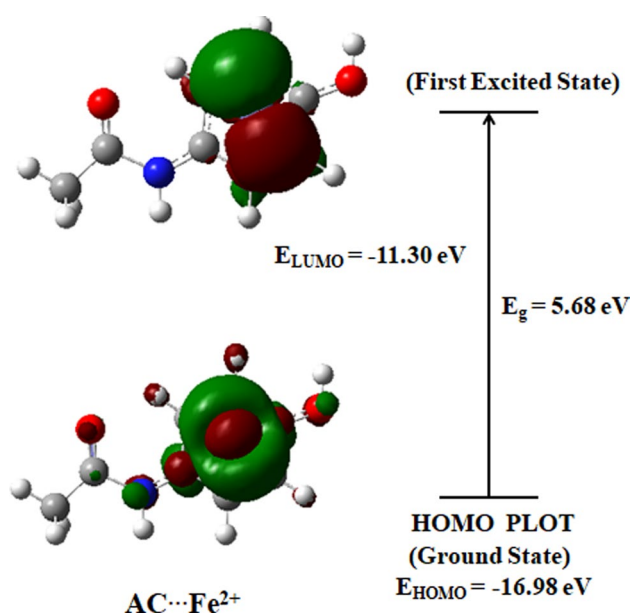


Fig. 5 HOMO and LUMO of $AC \cdots Fe^{2+}$ complex in the gas phase as obtained with M06-2X/6-311++G(d,p) level of theory

Table 7 Orbital energies (HOMO and LUMO), energy gap (E_g), hardness (η), electronic chemical potential (μ), electronegativity (χ) and electrophilicity index (ω) of $AC \cdots Fe^{2+}$ complex (in terms of eV) in the selected solvents

Media	E_{HOMO}	E_{LUMO}	E_g	η	μ	χ	ω
Water	-9.337	-2.261	7.076	3.538	-5.799	5.799	4.753
Methanol	-9.484	-2.458	7.027	3.513	-5.971	5.971	5.074
Ethanol	-9.562	-2.562	7.000	3.500	-6.062	6.062	5.250
Acetone	-9.630	-2.655	6.976	3.488	-6.143	6.143	5.409
Chloroform	-10.925	-4.339	6.586	3.293	-7.632	7.632	8.844
Ether	-11.131	-4.579	6.552	3.276	-7.855	7.855	9.417
Gas phase	-16.980	-11.296	5.684	2.842	-14.138	14.138	35.168

Some chemical concepts including energy gap (E_g), electronic chemical potential (μ) [89], chemical hardness (η) [90], electrophilicity index (ω) [91] and electronegativity (χ) [92] (χ is defined as the negative of μ , as follows: $\chi = -\mu$) known as global reactivity descriptors are listed in Table 7. These parameters are very significant, because they play a dominant role in describing the chemical reactivity and the kinetic stability of molecules. They are also computed from HOMO and LUMO energies by using Koopman's theorem equations [93], as given below:

$$\eta = \frac{(E_{LUMO} - E_{HOMO})}{2} \quad (3)$$

$$\mu = \frac{(E_{LUMO} + E_{HOMO})}{2} \quad (4)$$

where E_{HOMO} is the energy of Fermi level and E_{LUMO} is the first eigenvalue of valance band. The energy gap is indicated by energy difference between HOMO and LUMO. It is well known that the chemical hardness and softness of a molecule depend on the energy gap. Hard molecules have a large E_g and soft molecules have a small one. As given in Table 7, the values of E_g can be arranged, respectively, as: polar solvents > nonpolar solvents > gas phase. High E_g in the polar solvents indicates high stability and low reactivity of the AC complex. Table 7 shows that the energy gap of considered structure in the polar solvents does not change significantly. Hence, the stability of AC complex in these solvents is negligible. It can also be stated that the most stable structures have the highest chemical hardness. Our outcomes display that the AC complex establishes more hardness values in the polar solvents with respect to the other cases (see Table 7). Therefore, it can be concluded that the most reactive as well as the softest AC complex belongs to the gas phase.

The excellent linear relationships can be found between the energetic parameters and hardness. For instance, there are good correlations between the hardness values of complex (η) versus the ΔE and E_{stab} . The regression coefficients are equal to 0.972 and 0.991, respectively. The obtained relationships are shown using the following equations:

$$\eta = 0.0008 \Delta E + 3.501$$

$$\eta = -0.0698 E_{\text{stab}} + 2.8187$$

It is clear that by increasing the hardness, the binding energy diminishes and the stability enhances. For the studied complex, a direct relation is also found among electronic chemical potential and hardness. The outcomes demonstrate that the chemical potential values of the AC complex in both the gas phase and solution are negative; thus, all of them are stable (see Table 7). Besides, the AC complex reveals the most electronegativity value in the gas phase. Hence, it is the best electron acceptor in this phase.

The electrophilicity index has become an influential tool for the study of the reactivity of organic molecules participating in polar reactions [94, 95]. It encompasses the tendency of an electrophile to obtain an extra amount of electron density from the environment. The equation of electrophilicity index is given as follows:

$$\omega = \frac{\mu^2}{2\eta} \quad (5)$$

The electrophilicity index (ω) permits the categorization of organic compounds as strong electrophiles with $\omega > 1.5$ eV, moderate electrophiles with $0.8 < \omega < 1.5$ eV and marginal electrophiles with $\omega < 0.8$ eV [96]. Table 7 shows that the maximum and minimum values of the electrophilicity index for the AC complex belong to the gas phase and the water solvent, respectively.

The molecular electrostatic potential (MEP) at a point around a molecule gives an indication of the net electrostatic effect produced at that point by the total charge distribution (electron + proton) of the molecule. The importance of MEP lies in the fact that it simultaneously displays molecular size, shape as well as positive, negative and neutral electrostatic potential regions in terms of color grading (see Fig. 6). In the MEP map, the red and blue colors correspond to the regions of the maximum negative and positive potentials and green color represents regions of zero potential.

In the present study, MEP 3D plot of the AC...Fe²⁺ complex is drawn in Fig. 6. As shown in this figure, the electronegative oxygen atom is placed in negative potential area and the positive potential site is around the Fe²⁺ cation and the plane of the aromatic ring. The negative (red and yellow color) regions of MEPs are related to electrophilic reactivity, and the positive regions (blue color) are related to nucleophilic reactivity. Hence, it can be stated that the strongest attraction and repulsion sites belong to Fe²⁺ cation and oxygen atoms, respectively.

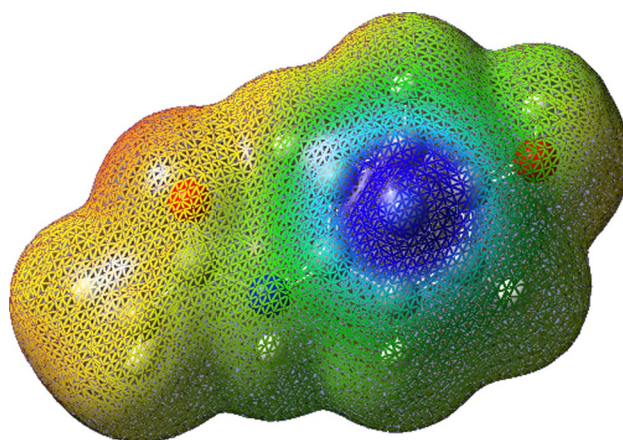


Fig. 6 Electron density isosurface for AC...Fe²⁺ complex calculated by M06-2X method and 6-311++G(d,p) basis set

4 Conclusions

In the present study, DFT calculations are performed to investigate the non-covalent interactions and to evaluate the cation- π interaction effect on the strength and nature of intramolecular H-bond in the AC complex. Based on PCM results, the calculated energies considerably change in the presence of different solvents. Our computations show that the interaction strength of complex in the gas phase is more than the solution phase, and in the polar solvents, it is lower than the nonpolar ones. Hence, the stability of studied complex increases in the solution phase in comparison with the gas phase. The AIM and NBO analyses are also employed to gain further insight into the established interactions in complex. The electron density properties demonstrate that the AC complex has specification of the closed-shell interactions in nature. Charge transfer values calculated by the NBO method reveal the highest charge transfer for the nonpolar solvents and the lowest that for the polar ones. Our findings also show that the H-bond of studied complex is placed in the weak H-bond category. According to the obtained results, the intramolecular H-bond is strengthened by the cation- π interaction, so that the AC complex in the gas phase has a stronger influence on the H-bond with respect to the solution phase. The analysis of frontier molecular orbitals is also used to evaluate some chemical concepts such as energy gap, chemical hardness and softness. Comparison of these parameters can play vital role in stabilizing the selected complex. High energy gap in the polar solvents indicates high stability and low reactivity of the AC system with respect to the other cases. On the other hand, the most reactive as well as the softest AC complex belongs to the gas phase.

Acknowledgements The support of this work by Vali-e-Asr University of Rafsanjan is acknowledged.

Compliance with ethical standards

Conflict of interest No potential conflict of interest was reported by the authors.

References

- Peter JZ, Pharm D, Edward PK, Pharm D, ABAT (1991) Treatment of acetaminophen overdose. *Am J Health Syst Pharm* 56:1081–1091
- Lee WM (2017) Acetaminophen (APAP) hepatotoxicity—Isn't it time for APAP to go away? *J Hepatol* 67:1324–1331
- Mangus BC, Miller MG (2005) Pharmacology application in athletic training. F.A Davis Company, Philadelphia
- Hamilton RJ (2013) Tarascon pocket pharmacopoeia: 2013 classic shirt-pocket edition. Jones & Bartlett Learning, Burlington
- McKay GA, Walters MR (2013) Clinical pharmacology and therapeutics. Wiley, Hoboken
- Ghanem CI, Pérez MJ, Manautou JE, Mottino AD (2016) Acetaminophen from liver to brain: new insights into drug pharmacological action and toxicity. *Pharmacol Res* 109:119–131
- Viswanathan AN, Feskanich D, Schernhammer ES, Hankinson SE (2008) Aspirin, NSAID, and acetaminophen use and the risk of endometrial cancer. *Cancer Res* 68:2507–2513
- Larson AM, Polson J, Fontana RJ, Davern TJ, Lalani E, Hynan LS, Reisch JS, Schiødt FV, Ostapowicz G, ObaidShakil A, Lee WM (2005) Acetaminophen-induced acute liver failure: results of a United States multicenter, prospective study. *Hepatology* 42:1364–1372
- Ricciotti E, FitzGerald GA (2011) Prostaglandins and inflammation. *Arterioscler. Thromb Vasc Biol* 31:986–1000
- Hinz B, Cheremina O, Brune K (2008) Acetaminophen (paracetamol) is a selective cyclooxygenase-2 inhibitor in man. *FASEB J* 22:383–390
- Muller-Dethlefs K, Hobza P (2000) Noncovalent interactions: a challenge for experiment and theory. *Chem Rev* 100:143–167
- Masoodi HR, Bagheri S, Ranjbar M (2016) Theoretical study of cooperativity between hydrogen bond-hydrogen bond, halogen bond-halogen bond and hydrogen bond-halogen bond in ternary FX...diazine...XF (X=H and Cl) complexes. *Mol Phys* 114:3464–3474
- Samimi HA, Esrafil M, Mohammadian-Sabet F, Haddadi H (2015) Theoretical study on cooperative interplay between anion- π and chalcogen-bonding interactions. *Mol Phys* 113:1442–1450
- Nowroozi A, Roohi H, Sadeghi MS, Sheibaninia M (2011) The competition between the intramolecular hydrogen bond and π -electron delocalization in trifluoroacetylacetone—a theoretical study. *Int J Quantum Chem* 111:578–585
- Esrafil M, Yourdkhani S, Bahrami A (2013) Characteristics and nature of the halogen-bonding interactions between CCl₃F and ozone: a supermolecular and SAPT study. *Mol Phys* 111:3770–3778
- Nowroozi A, Roohi H, Poorsargol M, Mohammadzadeh Jahani P, Hajiabadi H, Raissi H (2011) N–H...S and S–H...N intramolecular hydrogen bond in β -thioaminoacrolein: a quantum chemical study. *Int J Quantum Chem* 111:3008–3016
- Oshovsky GV, Reinhoudt DN, Verboom W (2007) Supramolecular chemistry in water. *Angew Chem Int Ed* 46:2366–2399
- Saalfrank RW, Maid H, Scheurer A (2008) Supramolecular coordination chemistry: the synergistic effect of serendipity and rational design. *Angew Chem Int Ed* 47:8794–8824
- Steiner T (1997) Unrolling the hydrogen bond properties of C–H...O interactions. *Chem Commun* 8:727–734
- Steiner T, Desiraju R (1998) Distinction between the weak hydrogen bond and the van der Waals interaction. *Chem Commun* 8:891–892
- Kodama Y, Nishihata K, Nishio M, Nakagawa N (1977) Attractive interaction between aliphatic and aromatic systems. *Tetrahedron Lett* 18:2018–2105
- Hobza P, Havlas Z (2000) Blue-shifting hydrogen bonds. *Chem Rev* 100:4253–4264
- Umezawa Y, Tsuboyama S, Takahashi H, Uzawa J, Nishio M (1999) CH... π interaction in the conformation of organic compounds. A database study. *Tetrahedron* 55:10047–10056
- Ungaro R, Pochini A, Andreetti GD, Sangermano V (1984) Molecular inclusion in functionalized macrocycles. Part 8. The crystal and molecular structure of calix[4]arene from phenol and its (1: 1) and (3: 1) acetone clathrates. *J Chem Soc Perkin Trans 2(12)*:1979–1985
- Kobayashi K, Asakawa Y, Kato Y, Aoyama Y (1992) Complexation of hydrophobic sugars and nucleosides in water with tetrasulfonate derivatives of resorcinol cyclic tetramer having a polyhydroxy aromatic cavity: importance of guest-host CH- π interaction. *J Am Chem Soc* 114:10307–10313
- Cubero E, Luque FJ, Orozco M (1998) Is polarization important in cation- π interactions? *Proc Natl Acad Sci* 95:5976–5980
- Ma JC, Dougherty DA (1997) The cation- π interaction. *Chem Rev* 97:1303–1324
- Lehn JM (1995) Supramolecular chemistry: concepts and perspectives. VCH Weinheim, Berlin
- Steed JW, Atwood JL (2000) Supramolecular chemistry. Wiley, West Sussex
- Fischer E, Dtsch B (1894) Einfluss der Configuration auf die Wirkung der Enzyme. *Chem Ges* 27:2985–2993
- Rooman M, Liévin J, Buisine E, Wintjens R (2002) cation- π /H-bond stair motifs at protein-DNA interfaces. *J Mol Biol* 319:67–76
- Starellas C, Escudero D, Frontera A, Quiñero D, Deyà PM (2009) Theoretical ab initio study of the interplay between hydrogen bonding, cation- π and π - π interactions. *Theor Chem Account* 122:325–332
- Escudero D, Frontera A, Quiñero D, Deyà PM (2008) Interplay between cation- π and hydrogen bonding interactions. *Chem Phys Lett* 456:257–261
- Yong-gan Y, Wen-jing S, Guo-rui F, Fu-de R, Yong W (2012) A B3LYP and MP2 (full) theoretical investigation on the cooperativity effect between cation-molecule and hydrogen-bonding interactions in the O-cresol complex with Na⁺. *Comput Theor Chem* 996:91–102
- Qingzhong L, Wenzuo L, Jianbo C, Baoan G, Jiazhong S (2008) Effect of methyl group on the cooperativity between cation- π interaction and NH...O hydrogen bonding. *J Mol Struct Theochem* 867:107–110
- Garcia-Raso A, Albertí F M, Fiol JJ, Tasada A, Barceló-Oliver M, Molins E, Escudero D, Frontera A, Quiñero D, Deyà PM (2007) Anion- π interactions in bisadenine derivatives: a combined crystallographic and theoretical study. *Inorg Chem* 46:10724–10735
- Greenaway F (1995) Structural aspects of metal ion-drug interactions, handbook of metal-ligand interactions in biological fluids, bioinorganic chemistry. Marcel Dekker, New York
- Ai H, Bu Y, Li P, Li Z, Hu X, Chen Z (2005) Geometry and binding properties of different multiple-state glycine-Fe⁺/Fe²⁺ complexes. *J Phys Org Chem* 18:26–34
- Banu L, Blagojevic V, Bohme DK (2012) Dissociation of deprotonated glycine complexes with Pb²⁺ and five transition-metal

- dications (Fe^{2+} , Co^{2+} , Ni^{2+} , Cu^{2+} , Zn^{2+}): the importance of metal bond activation. *Int J Mass Spectrom* 330–332:168–173
40. Marino T, Toscano M, Russo N, Grand A (2006) Structural and electronic characterization of the complexes obtained by the interaction between bare and hydrated first-row transition-metal ions (Mn^{2+} , Fe^{2+} , Co^{2+} , Ni^{2+} , Cu^{2+} , Zn^{2+}) and glycine. *J Phys Chem B* 110:24666–24673
 41. Rodgers MT, Armentrout PB (2004) A thermodynamic, “vocabulary” for metal ion interactions in biological systems. *Acc Chem Res* 37:989–998
 42. Campbell NRC, Hasinoff BB (1991) Iron supplements: a common cause of drug interactions. *Br J Clin Pharm* 31:251–255
 43. Mohamed Issa M, Mahmoud Nejmer R, Abu Shanab A (2013) Effects of iron on the pharmacokinetics of paracetamol in saliva. *Pak J Biol Sci* 16:2050–2053
 44. Moffat AC, Osselton MD, Widdop B, Watts J (2011) Clarkes analysis of drug and poisons. Pharmaceutical Press, London
 45. Sunagane N, Yoshibu E, Murayama N, Terawaki Y, Uruno T (2005) Simple method for precognitions of drug interaction between oral iron and phenolic hydroxyl group-containing drugs. *Yakugaku Zasshi* 125:197–203
 46. Campbell NA, Hasinoff B (1989) Ferrous sulfate reduces levodopa bioavailability: chelation as a possible mechanism. *Clin Pharmacol Therapeut* 45:220–225
 47. Campbell NRC, Rankine D, Goodridge AE, Hasinoff BB, Kara M (1991) Sienemet-ferrous sulphate interaction in patients with Parkinson disease. *Br J Clin Pharmacol* 30:559–605
 48. Demircan ÇA, Bozkaya U (2017) Transition metal cation– π interactions: complexes Formed by Fe^{2+} , Co^{2+} , Ni^{2+} , Cu^{2+} , and Zn^{2+} binding with benzene molecules. *J Phys Chem A* 121(34):6500–6509
 49. Yi HB, Lee HM, Kim KS (2009) Interaction of benzene with transition metal cations: theoretical study of structures, energies, and IR spectra. *J Chem Theory Comput* 5:1709–1717
 50. Molina JM, Dobado JA, Melchor S (2002) Structural and electronic effects of the interaction of metal cations with benzene. *J Mol Struct (Theochem)* 589–590:337–347
 51. Kolakkandy S, Pratihari S, Aquino AJA, Wang H, Hase WL (2014) Properties of complexes formed by Na^+ , Mg^{2+} , and Fe^{2+} binding with benzene molecules. *J Phys Chem A* 118:9500–9511
 52. Frisch MJ, Trucks GW, Schlegel HB, Scuseria GE, Robb MA, Cheeseman JR, Montgomery JA Jr, Vreven T, Kudin KN, Burant JC, Millam JM, Iyengar SS, Tomasi J, Barone V, Mennucci B, Cossi M, Scalmani G, Rega N, Petersson GA, Nakatsuji H, Hada M, Ehara M, Toyota K, Fukuda R, Hasegawa J, Ishida M, Nakajima T, Honda Y, Kitao O, Nakai H, Klene M, Li X, Knox JE, Hratchian HP, Cross JB, Bakken V, Adamo C, Jaramillo J, Gomperts R, Stratmann RE, Yazyev O, Austin AJ, Cammi R, Pomelli C, Ochterski JW, Ayala PY, Morokuma K, Voth GA, Salvador P, Dannenberg JJ, Zakrzewski VG, Dapprich S, Daniels AD, Strain MC, Farkas O, Malick DK, Rabuck AD, Raghavachari K, Foresman JB, Ortiz JV, Cui Q, Baboul AG, Clifford S, Cioslowski J, Stefanov BB, Liu G, Liashenko A, Piskorz P, Komaromi I, Martin RL, Fox DJ, Keith T, Al-Laham MA, Peng CY, Nanayakkara A, Challacombe M, Gill PMW, Johnson B, Chen W, Wong MW, Gonzalez C, Pople JA (2003) Gaussian 03 (Revision A.7). Gaussian Inc., Pittsburgh
 53. Zhao Y, Truhlar DG (2008) The M06 suite of density functionals for main group thermochemistry, thermochemical kinetics, noncovalent interactions, excited states, and transition elements. *Theor Chem Acc* 120:215–241
 54. Zhao Y, Schultz NE, Truhlar DG (2005) Exchange-correlation functional with broad accuracy for metallic and nonmetallic compounds, kinetics, and noncovalent interactions. *J Chem Phys* 123:161103-1–161103-4
 55. Zhao Y, Schultz NE, Truhlar DG (2006) Design of density functionals by combining the method of constraint satisfaction with parametrization for thermochemistry, thermochemical kinetics, and noncovalent interactions. *J Chem Theory Comput* 2:364–382
 56. Zhao Y, Truhlar DG (2006) A new local density functional for main-group thermochemistry, transition metal bonding, thermochemical kinetics, and noncovalent interactions. *J Chem Phys* 125:194101-1–194101-18
 57. Zhao Y, Truhlar DG (2007) Density functionals for noncovalent interaction energies of biological importance. *J Chem Theory Comput* 3:289–300
 58. Miertus S, Scrocco E, Tomasi J (1981) Electrostatic interaction of a solute with a continuum: a direct utilization of AB initio molecular potentials for the prevision of solvent effects. *Chem Phys* 55:117–129
 59. Espinosa E, Molins E (2000) Retrieving interaction potentials from the topology of the electron density distribution: the case of hydrogen bonds. *J Chem Phys* 113:5686–5694
 60. Boys SF, Bernardi F (1970) The calculation of small molecular interactions by the differences of separate total energies. Some procedures with reduced errors. *Mol Phys* 19:553–566
 61. Bader RFW (1990) Atoms in molecules: a quantum theory. Oxford University Press, Oxford
 62. BieglerKönig F, Schönbohm J (2002) Update of the AIM2000-program for atoms in molecules. *J Comput Chem* 23:1489–1494
 63. Reed AE, Curtiss LA, Weinhold F (1988) Intermolecular interactions from a natural bond orbital, donor-acceptor viewpoint. *Chem Rev* 88:899–926
 64. Glendening ED, Reed AE, Carpenter JE, Weinhold F (2003) NBO, version 3.1 (in). Gaussian, Inc., Pittsburg, CT
 65. Yoosefian M, Ansarinik Z, Etminan N (2016) Density functional theory computational study on solvent effect, molecular conformations, energies and intramolecular hydrogen bond strength in different possible nano-conformers of acetaminophen. *J Mol Liq* 213:115–121
 66. Marshall MS, Steele RP, Thanthirawatte KS, Sherrill CD (2009) Potential energy curves for cation– π interactions: off-axis configurations are also attractive. *J Phys Chem A* 113:13628–13632
 67. Bader RFW (1991) A quantum theory of molecular structure and its applications. *Chem Rev* 91:893–928
 68. Feynman RP (1939) Forces in molecules. *Phys Rev* 56:340–343
 69. Grabowski SJ, Sokalski WA, Dyguda E, Leszczyński J (2006) Quantitative classification of covalent and noncovalent H-bonds. *J Phys Chem B* 110:6444–6446
 70. Espinosa E, Souhassou M, Lachekar H, Lecomte C (1999) Topological analysis of the electron density in hydrogen bonds. *Acta Crystallogr B* 55:563–572
 71. Abramov YA (1997) On the possibility of kinetic energy density evaluation from the experimental electron-density distribution. *Acta Crystallogr A* 53:264–272
 72. Carroll MT, Chang C, Bader RFW (1988) Prediction of the structures of hydrogen-bonded complexes using the Laplacian of the charge density. *Mol Phys* 63:387–405
 73. Carroll MT, Bader RFW (1988) An analysis of the hydrogen bond in BASE-HF complexes using the theory of atoms in molecules. *Mol Phys* 65:695–722
 74. Vijayakumar S, Kolandaivel P (2005) Red-shifted and improper blue-shifted hydrogen bonds in dimethyl ether (DME) $_n$ ($n = 1–4$) and hydrated (DME) $_n$ ($n = 1–4$) clusters: a theoretical study. *J Mol Struct* 734:157–169
 75. Koch U, Popelier PLA (1995) Characterization of C–H–O hydrogen bonds on the basis of the charge density. *J Phys Chem* 99:9747–9754
 76. Popelier PLA (1998) Characterization of a dihydrogen bond on the basis of the electron density. *J Phys Chem A* 102:1873–1878

77. Gálvez O, Gómez PC, Pacio LF (2003) Variation with the intermolecular distance of properties dependent on the electron density in cyclic dimers with two hydrogen bonds. *J Chem Phys* 118:4878–4895
78. Domagala M, Grabowski SJ (2005) CH...N and CH...S hydrogen bonds. Influence of hybridization on their strength. *J Phys Chem A* 109:5683–5688
79. Raissi H, Yoosefian M, Moshfeghi E, Farzad F (2012) Theoretical study on β -aminoacroleine; density functional theory, atoms in molecules theory and natural bond orbitals studies. *J Chem Sci* 124:731–739
80. Raissi H, Yoosefian M, Khoshkhou S (2012) Conformational study of the (z) -[(2-iminoethylidene) silyl] amine at the MP2, DFT and G2MP2 levels. *Comput Theor Chem* 983:1–6
81. Raissi H, Yoosefian M, Zamani S, Farzad F (2012) Conformational study, molecular structure, and S...H–N, S–H...N intramolecular hydrogen bond in thioformyl-3-aminoacrylaldehyde. *J Sulfur Chem* 33:75–85
82. Raissi H, Jalbout A, Yoosefian M, Fazli M, Nowroozi A, Shahinin M, De Leon A (2010) Intramolecular hydrogen bonding in structural conformers of 2-amino methylene malonaldehyde: AIM and NBO studies. *Int J Quantum Chem* 110:821–830
83. Fukui K, Yonezawa T, Shingu H (1952) A molecular orbital theory of reactivity in aromatic hydrocarbons. *J Chem Phys* 20:722–725
84. Saikia N, Deka RC (2010) Theoretical study on pyrazinamide adsorption onto covalently functionalized (5,5) metallic single-walled carbon nanotube. *Chem Phys Lett* 500:65–70
85. Fukui K (1982) Role of Frontier orbitals in chemical reactions. *Science* 218:747–754
86. Sajan D, Lakshmi KU, Erdogdu Y, Joe IH (2011) Molecular structure and vibrational spectra of 2,6-bis(benzylidene)cyclohexanone: a density functional theoretical study. *Spectrochim Acta* 78:113–121
87. Ibrahim M, Mahmoud AA (2009) Computational notes on the reactivity of some functional groups. *J Comput Theor Nanosci* 6:1523–1526
88. Ibrahim M, El-Haes H (2005) Computational spectroscopic study of copper, cadmium, lead and zinc interactions in the environment. *Int J Environ Pollut* 23:417–424
89. Chattaraj PK, Poddar A (1999) Molecular reactivity in the ground and excited electronic states through density-dependent local and global reactivity parameters. *J Phys Chem A* 103:8691–8699
90. Pearson RG (1997) Chemical hardness-applications from molecules to solids. VCH-Wiley, Weinheim
91. Parr RG, Szentpály LV, Liu S (1999) Electrophilicity index. *J Am Chem Soc* 121:1922–1924
92. Sen KD, Jorgensen CK (1987) Electronegativity, structure and bonding. Springer, New York
93. Koopmans T (1933) Über die Zuordnung von Wellenfunktionen und Eigenwerten zu den einzelnen Elektronen eines atoms. *Physica* 1:104–113
94. Pérez P, Domingo LR, Aizman A, Contreras R (2007) The electrophilicity index in organic chemistry. In: Theoretical aspects of chemical reactivity. Elsevier, New York
95. Domingo LR, Ríos-Gutiérrez M, Pérez P (2016) Applications of the conceptual density functional theory indices to organic chemistry reactivity. *Molecules* 21:748-1–748-22
96. Domingo LR, Aurell MJ, Pérez P, Contreras R (2002) Quantitative characterization of the global electrophilicity power of common diene/dienophile pairs in Diels–Alder reactions. *Tetrahedron* 58:4417–4423

Publisher's Note Springer Nature remains neutral with regard to jurisdictional claims in published maps and institutional affiliations.